ARTICLES: PROCESS SENSING AND CONTROL

Ionic-Complementary Peptide-Modified Highly Ordered Pyrolytic Graphite Electrode for Biosensor Application

Hong Yang and Shan-Yu Fung
Dept. of Chemical Engineering, University of Waterloo, Waterloo, ON, Canada N2L 3G1

Wei Sun
Dept. of Chemical and Materials Engineering, University of Alberta, Edmonton, AB, Canada T6G 2G6

Susan Mikkelsen
Dept. of Chemistry, University of Waterloo, Waterloo, ON, Canada N2L 3G1

Mark Pritzker and P. Chen
Dept. of Chemical Engineering, University of Waterloo, Waterloo, ON, Canada N2L 3G1

DOI 10.1021/bp.1
Published online in Wiley InterScience (www.interscience.wiley.com).

Ionic-complementary peptides are promising new biomaterials with potential applications in bionanotechnology. In the present investigation, a typical ionic-complementary peptide, EFK16-II, was used to modify a highly ordered pyrolytic graphite (HOPG) electrode. Upon modification, peptide nanofibers, parallel or oriented 60° or 120° to each other, were formed on the surface of HOPG electrode. Surface wettability of the electrode was improved as indicated by a significant decrease in the water contact angle. The electrochemical response of the EFK16-II nanofiber-modified HOPG electrode for the ferricyanide/ferrocyanide redox couple was characterized. Cyclic voltammograms indicated that the presence of peptide nanofibers on the HOPG electrode did not block electron transfer at slow scan rates (∼2 mV/s), but did so at high scan rates (∼ 100 mV/s). A model enzyme glucose oxidase (GOx) was covalently immobilized onto this nanofiber-modified electrode, and its potential as an enzyme-based biosensor for glucose was examined. At an applied potential of +0.45 V (vs. Ag/AgCl), the current increased linearly with glucose concentration up to 7.5 mM and a relative high sensitivity was obtained at 11.3 ± 1.0 nA/(mM mm^2). The immobilized GOx showed high affinity for glucose, with a Michaelis–Menten constant K_m of 6.8 ± 0.9 mM. It also exhibited relatively good storage and operational stabilities, and reflected in only a small decrease (13%) in the current response after 1 month storage and negligible changes upon 50 cyclic voltammetric scans. The results presented here demonstrate an excellent potential of the use of ionic-complementary peptides to modify electrode surfaces for biomolecular sensing and diagnostics.
Keywords: ionic-complementary peptide, (bio)molecular sensing, surface modification, patterned nanofibers

Introduction

Biosensors are analytical devices that combine a biologically sensitive element (biorecognition agent) with a physical or chemical transducer (e.g., noble metal or graphite electrode, optical fibers, surface acoustic wave, or calorimetric devices) to selectively detect and measure the amount of specific compounds in a given external environment.[1] They have been widely used in the biomedical diagnostics field and the food industry. Rapid and reliable detection of specific nucleic acid sequences, proteins (e.g., antibodies and antigens), cell-surface markers, and pathogens is essential in biomedical works such as diagnosis of diseases, high-throughput assays, drug development as well as unraveling complexities of cellular chemical networks.[2–5] In the food industry, applications of biosensors range from testing pesticide residues to the routine determination of analyte concentrations including glucose, sucrose, and alcohol, which can be indicators of food quality/acceptability.[6] Therefore, intense efforts have been placed on the research and development of novel biosensing devices that are sensitive, stable, portable, easy to use, and inexpensive to operate.

Correspondence concerning this article should be addressed to P. Chen at p4chen@cape.uwaterloo.ca.

The key element in the design of a suitable sensor architecture is the immobilization of a specific biological recognition element such as an enzyme on the transducer surface.[7] Suitable surface linkers or matrices are therefore required to immobilize the enzyme on the surface and provide a biocompatible platform to allow the enzyme to function properly and effectively. With rapid developments in nanotechnology, materials scientists, and chemists are now focusing on using various nanoscale material assemblies for such a purpose.

Among the many nanoassemblies, self-assembled monolayers (SAMs) containing functional groups and terminated by thiols have been widely used as linkers for the immobilization of many enzymes on gold electrodes.[8–11] The covalent immobilization of enzymes via SAMs can increase the binding capacity of the electrode surface toward enzymes and provide molecular level control over the enzyme distribution on the electrode surface.[12] In addition, undesired Faradaic background currents can be suppressed because of the insulating effect of the SAM on electron transfer. However, current for the desired redox reactions may also be suppressed, resulting in lower responses.[13] The use of SAM linkers is also limited by the fact that thiols tend to reductively desorb from gold electrodes at potentials below −1.0 V (vs. SCE), thereby narrowing the working potential window.[14]

Recently, self-assembled nanotubes of the peptide diphenylalanine (FF) have shown potential for use in biosensor applications.[15,16] Modification of carbon and gold electrodes by these peptide nanotubes can improve the reaction reversibility of the $Fe(CN)_6^{4-}/Fe(CN)_6^{3-}$ redox couple and the electrochemical fingerprint of the electrode; it also enables these electrodes to exhibit a direct and unmediated response to hydrogen peroxide and NADH. In addition, glucose oxidase (GOx)-based biosensors modified by such peptide nanotubes have been shown to exhibit unmediated, rapid responses to successive additions of glucose. However, problems remain with the storage stability of these types of enzymatic biosensors.

The promise of dipeptide nanotubes for biosensor applications has encouraged us to explore a special class of ionic-complementary, self-assembling peptides. These new peptides have a unique sequence of alternating hydrophobic and hydrophilic residues, imparting them with amphiphilic characteristics. They can self-assemble into stable β-sheet-rich nanofibers and macroscopic membranes in aqueous solution.[17,18] In particular, one member of this class of peptides has been found to assemble into nanofibers on both hydrophilic and hydrophobic surfaces under pH-controlled conditions.[19,20] The nanostructures assembled from these peptides have shown promise for a variety of uses, such as surface modification, tissue scaffolding, and drug delivery.[17,20–28]

Further research in surface modification is now primarily focused on the development of an ionic-complementary peptide-based platform for (bio)molecular sensing. The presence of ionic-complementary peptide assemblies on an electrode surface may not only provide functional groups to immobilize enzymes onto the electrode surface but also improve the surface biocompatibility, optimizing the enzyme functions. Accordingly, the activity and stability of the immobilized enzymes may be improved.

In this study, GOx was used as a model enzyme to demonstrate an amperometric biosensor for glucose, using a HOPG electrode modified by the ionic-complementary peptide EFK16-II (Figure 1). To understand the conformation of the peptide used, Fourier transform infrared spectroscopy (FTIR) was applied to elucidate the peptide secondary structure. The peptide nanostructures assembled on HOPG were observed with atomic force microscopy (AFM) imaging. The hydrophobicity or wettability of the peptide-modified electrode was characterized by water contact angle measurements. Finally, a series of electrochemical methods was employed to characterize the peptide-modified electrode and to test the activity and stability of the enzyme immobilized.

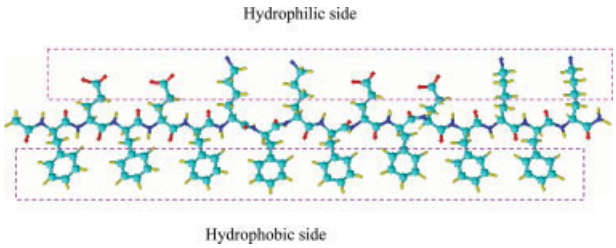

Figure 1. Molecular structure of EFK16-II.

Materials and Methods

Materials

The ionic-complementary peptide EFK16-II ($C_{70}H_{121}N_{21}O_{25}$, molecular weight 2,265.6 g/mol) has the sequence FEFEFKFKFEFEFKFK (Figure 1), where F corresponds to phenylalanine, E to glutamic acid, and K to lysine. At neutral pH, F is neutral, while E and K are negatively and positively charged, respectively. This peptide was purchased from CanPeptide Inc. (Quebec, Canada) and used without further purification. The N-terminus and C-terminus of the peptide were protected by acetyl and amino groups, respectively.

Highly ordered pyrolytic graphite (HOPG, ZYB grade) was obtained from SPI Supplies (West Chester, PA). GOx (EC 1.1.3.4 type X-S, from *Aspergillus niger*), glucose, 1-ethyl-3-(3-dimethylaminopropyl) carbodiimide (EDC), *N*-hydroxysulfosuccinimide (NHS), ferrocenecarboxylic acid (FCA), and potassium ferricyanide were all purchased from Sigma-Aldrich (Oakville, ON, Canada).

Fourier transform infrared spectroscopy

A FTIR was obtained over the range from 1,450–1,750 cm^{-1} to determine the secondary structure of the peptide in the assemblies. Examination of the amide I band (1,600–1,700 cm^{-1}) within this range enables distinction to be made between various secondary structures, e.g., α-helices, β-sheets, and random coils. Hundred microliters of 0.5 mg/mL EFK16-II (incubated for weeks to allow the formation of stable peptide assemblies) were placed on a crystal slide of calcium fluoride (CaF_2) and dried at room temperature. The FTIR spectra of the thin films were obtained at a wave number resolution of 4 cm^{-1} with a Bio-Rad spectrometer (FTS3000MX, EXCALIBUR series, Hercules, CA). The baseline was subtracted from the observed absorbance intensity and the resulting spectra normalized with respect to the maximum intensity.

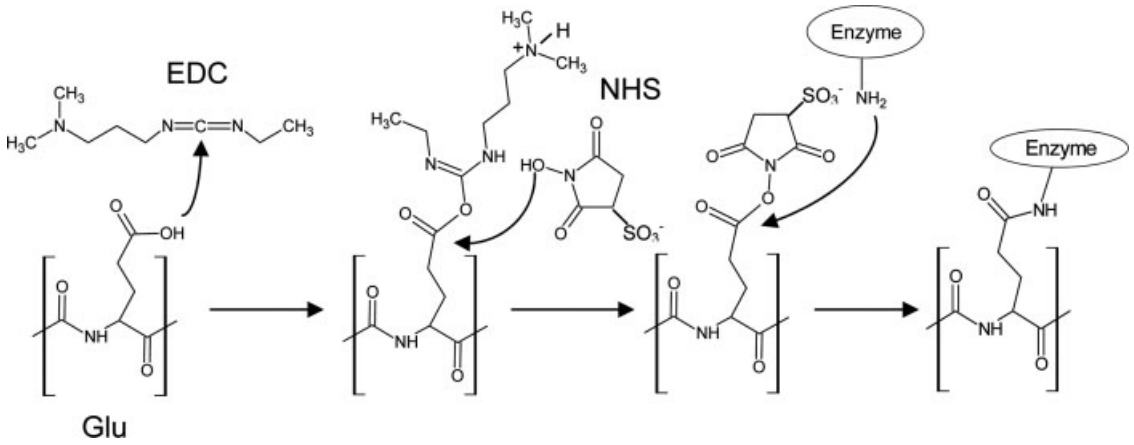

Figure 2. Covalent attachment of the enzyme GOx to the glutamic acid residue of EFK16-II using 1-ethyl-3-(3-dimethylaminopropyl) carbodiimide (EDC) and *n*-hydroxysulfosuccinimide (NHS).

Atomic force microscopy

Imaging of the peptide-modified HOPG surface was performed using a PicoScan™ AFM (Molecular Imaging, Phoenix, AZ) in 500 μL of pure water in an environmentally controlled chamber at room temperature (to minimize evaporation of the solution). A scanner with a maximum scan area of 6 $\times$ 6 μm^2 was used. Silicon nitride cantilevers with a nominal spring constant of 0.58 N/m (DNP-S, Digital Instruments, Santa Barbara, CA) and a tip radius of 10 nm were used for tapping mode operation. For the best imaging quality, the tapping frequency was typically set between 16 and 18 kHz and the scan rate was controlled at 0.857 lines/s. AFM images were obtained at a resolution of 256 $\times$ 256 pixels.

Contact angle measurements

Hundred microliters of 0.5 or 1.0 mg/mL EFK16-II solution were placed on a freshly cleaved HOPG surface for 3 or 5 h (as indicated in figure and table captions) and then washed with pure water three times before use. Contact angle measurements were then conducted to determine changes in the hydrophobicity of the surfaces upon EFK16-II modification. The contact angle measurements were made by manually depositing a sessile drop of water (30 μL) on either an unmodified or EFK16-II-modified surface placed inside a sealed, water-saturated chamber (to prevent water evaporation). A sequence of cross-sectional images of the sessile drop was recorded at 5-s intervals over a period of 5 min. The recorded images were analyzed by the Axisymmetric Drop Shape Analysis-Profile (ADSA-P) program[29] to yield the contact angle value. All the experiments were temperature-controlled by a refrigerated bath with a circulator digital controller (NESLAB Instrument, Inc., Georgetown, Ontario) to ensure that the temperature of the system remained at 20°C $\pm$ 0.1°C during the measurements. Static water contact angles for each surface are reported herein and represent the average of measured values obtained from three different samples.

Preparation of enzyme-immobilized electrode

Two hundred microliters of 0.5 mg/mL EFK16-II stock solution were injected onto the freshly cleaved surface of HOPG electrodes (2 cm $\times$ 2 cm) and incubated overnight to fabricate the EFK16-II-modified electrodes. The steps by which the enzyme electrode was prepared are shown in Figure 2.[30] The EFK16-II-modified electrode surfaces were first washed three times with pure water to remove loosely attached EFK16-II. The carboxylic acid groups of EFK16-II on the electrode were then activated with 200 μL of 50 mM potassium phosphate buffer (pH 5.5) containing 2 mM EDC and 5 mM NHS for 1 h at room temperature. This step converts the carboxylate group into its NHS ester, which is susceptible to attack by amines. Consequently, amide bonds form between the enzyme molecules and the glutamic acid residues of the peptide (Figure 2). After the activation, the electrodes were rinsed with a potassium phosphate buffer (pH 5.5) three times and immediately covered with 200 μL of 50 mM phosphate buffer (pH 5.5) containing 1 mg/mL GOx, and incubated overnight at 4°C. The enzyme electrode was then well rinsed several times with a potassium phosphate buffer (pH 7.0) and used immediately. Although not included here, results of control experiments suggest that small amounts of physically adsorbed enzyme may remain on the electrode even after rinsing several times with buffer solution.

Electrochemical measurements

All electrochemical measurements were conducted with a CHI650A Potentiostat (CH Instruments, Inc., Austin, TX). Cyclic voltammetry was carried out in a conventional three-electrode configuration, with the GOx-immobilized-EFK16-II-modified HOPG electrode (GOx/EFK16-II/HOPG, geometric area of 4 cm^2) as the working electrode, a platinum wire as the auxiliary electrode and Ag/AgCl (3 M NaCl, Bioanalytical Systems, West Lafayette, IN) as the reference electrode. All potentials reported herein correspond to the Ag/AgCl scale. The scans obtained in the presence of potassium ferricyanide proceeded cathodically from 0.5 V to 0 V before being reversed back to 0.5 V. The scans proceeded from 0.0 V to 0.5 V and back to 0.0 V when the GOx-immobilized-EFK16-II-modified HOPG electrode was used. The electrolyte was a 100 mM potassium phosphate buffer containing 0.2 mM FCA and various concentrations of glucose ranging from 0 to 20 mM (diluted from a stock solution prepared at least 24 h prior to use to allow mutarotation to

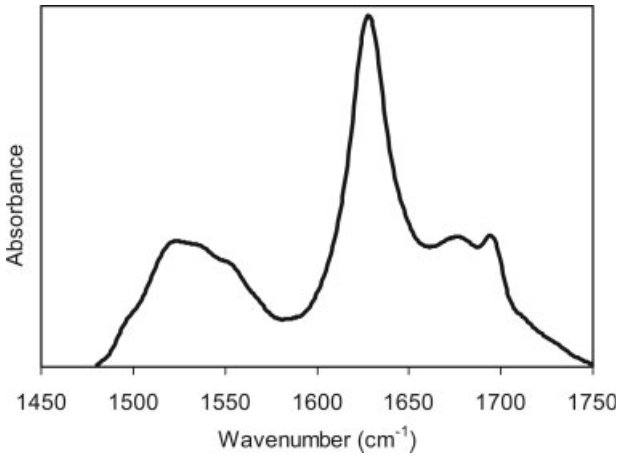

Figure 3. FTIR spectrum of EFK16-II.

occur). The activity of the immobilized GOx was tested by measuring the current response during cyclic voltammetry experiments in the presence of 20 mM glucose.

The Michaelis–Menten kinetic parameters (Michaelis–Menten constant K_m and the maximum amperometric response I_{max}) were obtained by fitting the equation $I = \frac{I_{max}[S]}{K_m+[S]}$ to the experimental data. K_m reflects the strength of the GOx-glucose interaction, while I_{max} corresponds to the maximum rate of the enzyme reaction at high glucose concentration when the amount of active enzyme on the electrode has reached saturation. In the equation given earlier, [S] is the bulk concentration of glucose.

Results and Discussion

Secondary structure of EFK16-II in the assemblies

To characterize the secondary structure of EFK16-II, FTIR spectroscopy was used to distinguish between β-sheets, α-helices, and random coils within the amide I band (1,600–1,700 cm^{-1}) caused by C=O stretching. Figure 3 shows a typical FTIR spectrum of the EFK16-II sample. A prominent characteristic band appears in the spectrum at about 1,628 cm^{-1}, which can be attributed to the formation of a β-sheet secondary structure.[31,32] This result demonstrates that the peptide self-assembles with a predominantly β-sheet secondary structure.

Characterization of the EFK16-II-modified HOPG electrode

Nanostructure of EFK16-II Assemblies on HOPG. Figures 4a,b shows the AFM images of the surfaces of bare HOPG and EFK16-II modified HOPG, respectively. After 3-h incubation of HOPG in 0.5 mg/mL EFK16-II, the formed nanofibers arranged either in parallel or at 60° or 120° to each other on the surface. The formation of patterned nanostructures on a HOPG surface has been previously observed, with many molecules ranging from alkyl chain-grafted fullerenes,[33] metal-organic complexes,[34] to peptides/proteins and polymers.[35–37] This formation process has been characterized as being surface directed/assisted assembly. Such orientations of the adsorbed molecules/nanofibers arise presumably due to the hexagonal crystal structure of the HOPG (001) surface and reflect the importance of substrate–peptide interactions.

The adsorption of EFK16-II on HOPG is likely due to hydrophobic interactions. As mentioned earlier, the peptide has an amphiphilic structure in which the hydrophobic phenylalanine residues lie on one side of the backbone, while the hydrophilic lysine and glutamic acid residues lie on the other side (Figure 1). When the peptide assembles in a β-strand arrangement, it can attach to a hydrophobic surface through hydrophobic interaction in which the phenylalanine side chain is oriented toward HOPG and the lysine and glutamic acid groups face the solution (Figure 4c). In the present case, the height of the patterned nanofibers on HOPG is estimated to be 0.8 ± 0.2 nm, which is comparable to that of a single β-sheet (~1.2 nm, estimated from Chemsketch software, Toronto, Canada). This suggests that each fiber is made up of only a single layer of β-sheet on the surface. Note that if such a structure forms, the EFK16-II-modified HOPG surface should be more hydrophilic than an unmodified HOPG surface, since the lysine and glutamic acid residues would be oriented outward into the solution.

Wettability of the EFK16-II-Modified HOPG Electrode. Water contact angle measurements were conducted to determine whether the hydrophobicity of the HOPG surface changes upon modification by EFK16-II. Figures 4d,e show photographs of the water sessile drops on the HOPG surface before and after EFK16-II modification. The water contact angle on a freshly cleaved HOPG surface is 71.4 ± 5.7° (Figure 4d), indicating that the surface is somewhat hydrophobic. Once the peptide solution has contacted the HOPG surface for 3 h and nanofibers allowed to form, the water contact angle decreases to about 36.9 ± 1.5°, indicating that the surface has become more hydrophilic (Figure 4e). This decrease is consistent with what would be expected from the proposed single layered β-sheet structure in which the peptide interacts with HOPG through its hydrophobic side and the lysine and glutamic acid residues are oriented toward the aqueous solution (Figure 4c).

The wettability of the EFK16-II-modified HOPG surface is found to vary with the peptide concentration and the incubation time of the EFK16-II solution on the HOPG surface. As shown in Table 1, an increase in the EFK 16-II concentration from 0.5 to 1.0 mg/mL EFK16-II leads to a decrease in water contact angle from 36.9 ± 1.5° to 15.5 ± 2.6° after 3-h incubation. Similarly, with the same peptide concentration (0.5 mg/mL), an increase in the incubation time to 5 h results in a lower water contact angle of 14.7 ± 2.1°. This increase in hydrophilicity may be due to an increase in the surface coverage of EFK16-II on HOPG. It has previously been found that increases in peptide concentration and incubation time raise the coverage density of peptide assemblies on HOPG.[20]

Electrochemical Characterization of the EFK16-II-Modified HOPG Electrode. The electrochemical properties of the EFK16-II-modified HOPG electrodes were studied by obtaining cyclic voltammograms for the $Fe(CN)_6^{4-}/Fe(CN)_6^{3-}$ redox couple. Figure 5 shows cyclic voltammograms obtained on unmodified HOPG and EFK16-II-modified HOPG electrodes immersed in a solution containing 1.0 mM $K_3Fe(CN)_6$ in 0.1 M KCl at scan rates of 2 and 100 mV/s. At the scan rate of 2 mV/s (Figure 5a), the CVs of unmodified HOPG and EFK16-II-modified HOPG show similar well-behaved responses that are characteristic of the $Fe(CN)_6^{4-}/Fe(CN)_6^{3-}$ redox couple. This indicates that the presence of the EFK16-II nanofiber coating does not interfere with electron transfer to any significant extent when the potential is scanned slowly. The peak separation ($\Delta E_p = E_{pa}$

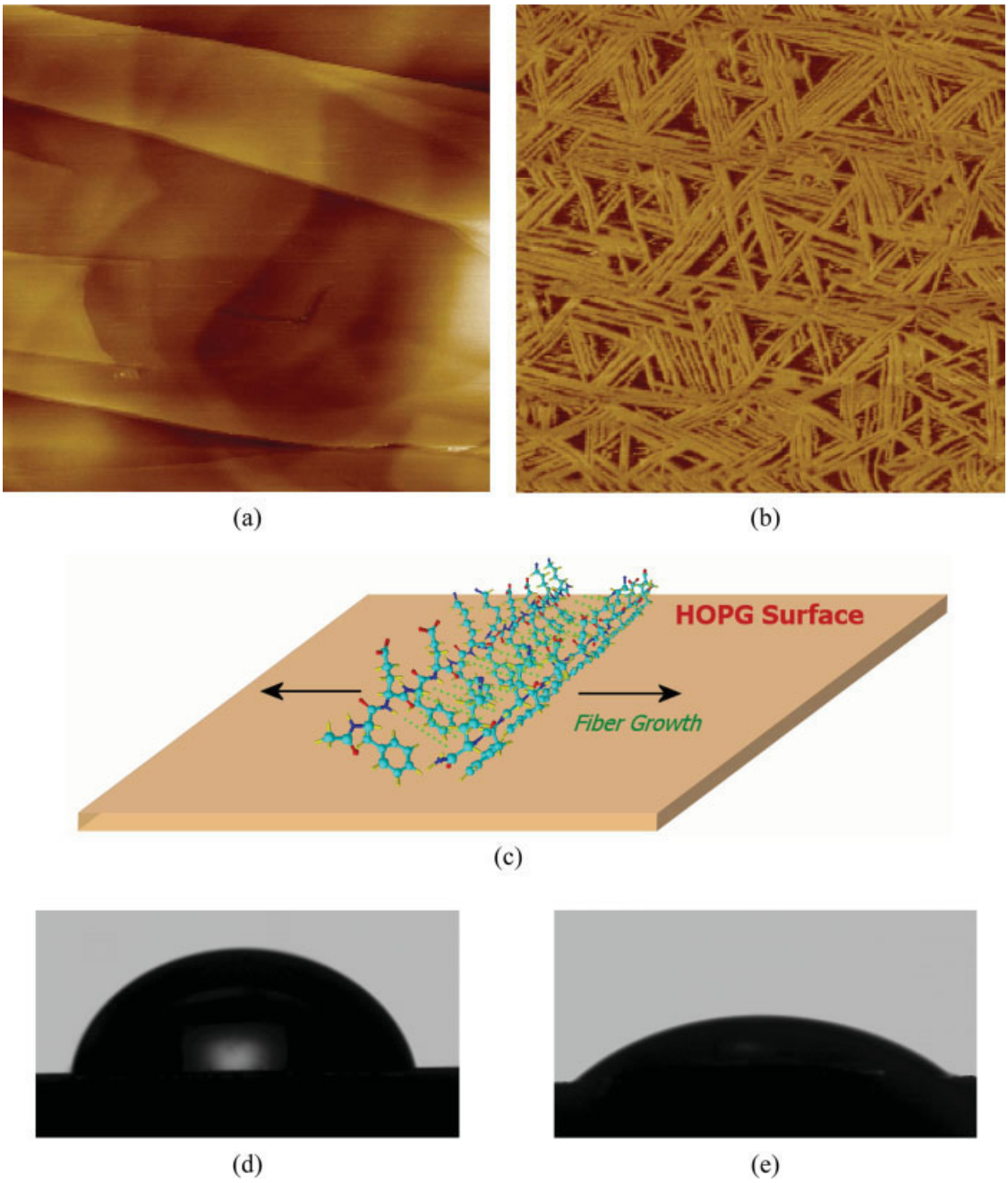

Figure 4. Liquid AFM images of HOPG (a) and 0.5 mg/mL EFK16-II-modified HOPG electrode for 3 h (b). Diagram of EFK16-II assembly on HOPG electrode (c). Photographs of water drop on HOPG (d) and 0.5 mg/mL EFK16-II modified HOPG electrode for 3 h (e). The AFM scan scale is 1,000 nm × 1,000 nm.

$- E_{pc}$) decreases slightly from 193 mV for the unmodified electrode to 185 mV for the electrode modified by EFK16-II. However, at the higher scan rate of 100 mV/s (Figure 5b), a dramatic difference is observed depending on whether or not the electrode is modified. Both cathodic and anodic peaks still appear during the forward and reverse scans obtained on the unmodified electrode. Comparison of the peak heights to the corresponding ones obtained at 2 mV/s (Figure 5a) also shows that their ratios are reasonably close to the value of $(100/2)^{1/2}$ expected when a process is controlled by diffusion of redox species involved in a reversible Nernstian reaction.[38] On the other hand, significant attenuation of both the cathodic and anodic currents is observed when the modified electrode is used at the higher scan rate. In fact, peaks no longer appear during the forward and reverse scans. The cathodic current during the forward scan and the anodic current during the reverse scan are suppressed considerably relative to that observed on the unmodified electrode. The results in Figures 5a,b provide evidence of the presence and good adhesion of the peptide assemblies to the electrode. They also show that the presence of the peptide assemblies increases the resistance

Table 1. Contact Angles Measured on HOPG and EFK16-II-Modified HOPG Surfaces at Different Peptide Concentrations and Incubation Times

Surfaces	Contact Angle
HOPG	71.4 ± 5.7°
0.5 mg/ml EFK/HOPG-3 h	36.9 ± 1.5°
0.5 mg/ml EFK/HOPG-5 h	14.7 ± 2.1°
1.0 mg/ml EFK/HOPG-3 h	15.5 ± 2.6°

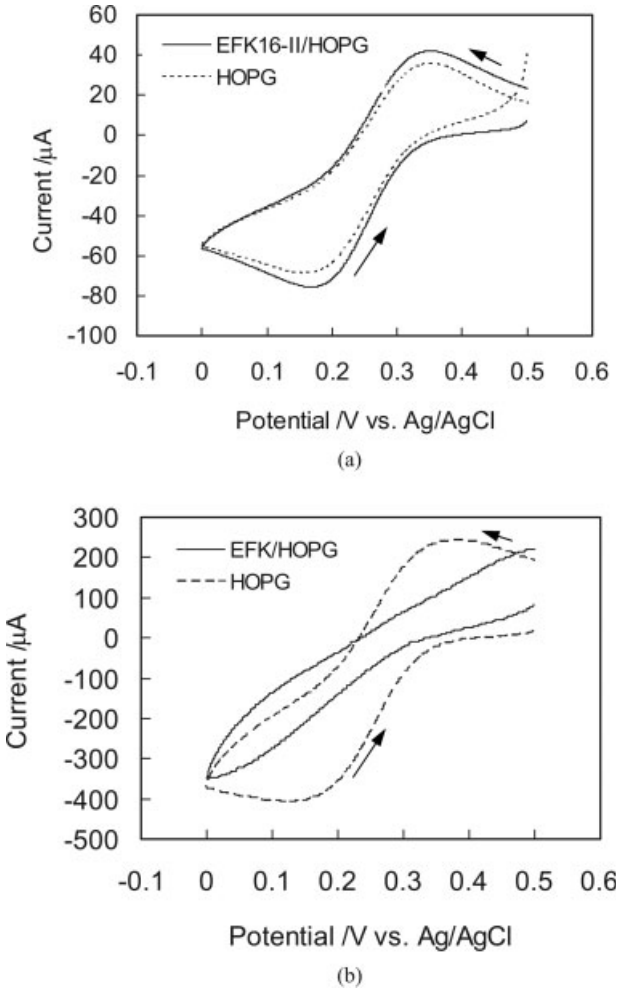

Figure 5. Cyclic voltammograms obtained in the presence of 1.0 mM $K_3Fe(CN)_6$ with 0.1 M KCl solution on bare HOPG (dotted line) and EFK16-II-modified HOPG electrodes (solid line) at a scan speed of 2 mV/s (a) and 100 mV/s (b).

Electrode area is 2 × 2 cm^2. The arrows indicate the scan direction.

to electron transfer relative to that on the unmodified HOPG. Moreover, the redox couple is able to overcome the barrier of the EFK16-II assemblies on the HOPG surface sites reasonably well at the low scan speed, but can no longer do so when the available time frame is reduced considerably by increasing the scan rate to 100 mV/s.

The height of peptide nanofiber assemblies (0.8 ± 0.2 nm) is less than the distance (1.5 nm) over which electron tunneling can occur.[38] Electron transfer between the electrode and the redox probe could occur by electron tunneling or by reaction at defect/pinhole sites on the peptide-modified HOPG electrode.

The electrochemical stability of the EFK16-II-modified HOPG electrode was tested by obtaining a cyclic voltammogram in 0.1 M KCl solution in the absence of ferricyanide. The absence of detectable redox peaks indicates that the peptide assemblies remain stable on the electrode over the potential range used.

Electrocatalytic oxidation of glucose

Figure 6 shows cyclic voltammograms of the GOx-immobilized EFK16-II-modified HOPG electrode in 0.1 M potassium phosphate buffer (pH 7.0) containing 0.2 mM FCA as a mediator[1] in the absence and presence of 20 mM glucose. In the absence of glucose, the characteristic and well-behaved voltammogram of FCA is observed (Figure 6a). In the presence of glucose, an electrocatalytic anodic current is observed (Figure 6b), indicating that GOx molecules are immobilized on HOPG and maintain their activity.[10]

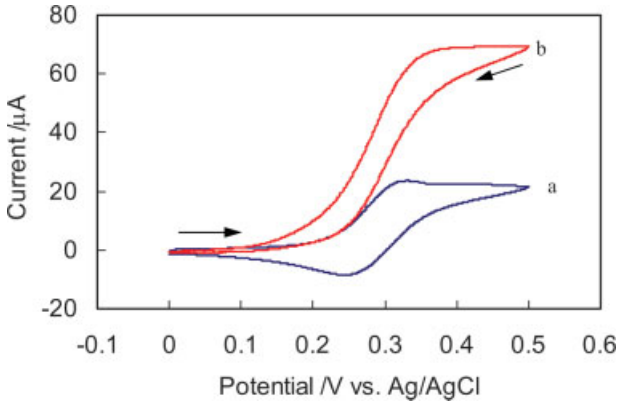

Figure 6. Cyclic voltammograms of the GOx-immobilized EFK16-II-modified HOPG electrode obtained in 100 mM potassium phosphate buffer (pH 7.0) containing 0.2 mM FCA before (a) and after (b) the addition of 20 mM glucose.

Scan rate = 2 mV/s; electrode area = 2 × 2 cm^2. The arrows indicate the scan directions.

To better characterize the fabricated ionic-complementary peptide-based enzyme electrode, a calibration curve was constructed from chronoamperometry data. *I-t* curves for the enzyme electrode shown in Figure 7a were acquired at a constant potential of 0.45 V in the presence of various concentrations of glucose. Steady-state currents were obtained within 2 min. The background-subtracted steady-state currents at various glucose concentrations were used to construct the calibration curve shown in Figure 7b. Anodic currents rise with increasing glucose concentration until they reach a plateau at high glucose concentrations, consistent with that expected from Michaelis–Menten kinetics.[10] The response is linear up to 7.5 mM glucose (Figure 7b inset), which covers the range of 3.5–6.5 mM required for clinical applications.[39]

The calibration curve shows good linearity over the glucose concentration range from 0 to 7.5 mM, with a coefficient of determination $r^2 = 0.96$. The data shown in Figure 7b were analyzed to determine the Michaelis–Menten kinetic parameters. The apparent Michaelis–Menten constant K_m value for the EFK16-II-based enzyme biosensor was found to be 6.8 ± 0.9 mM, which is much smaller than that reported for thiol and $CaCO_3$ nanoparticle-modified Pt electrodes (21–24 mM).[40,41] It should be noted that the smaller the value of K_m, the higher is the affinity of immobilized GOx for glucose. In addition, I_{max} and the sensitivity (the slope of the calibration curve in the linear range) were found to be 142.0 ± 7.3 nA mm^{-2} and 11.3 ± 1.0 nA/(mM mm^2), respectively. This I_{max} value is similar to the value of ~150 nA mm^{-2} obtained for gold electrodes modified with GOx and alkanethiol, whereas the obtained sensitivity is almost three times higher that obtained with GOx-modified thiol-modified gold nanotube and gold electrodes (~4 nA/(mM mm^{-2})).[42,43]

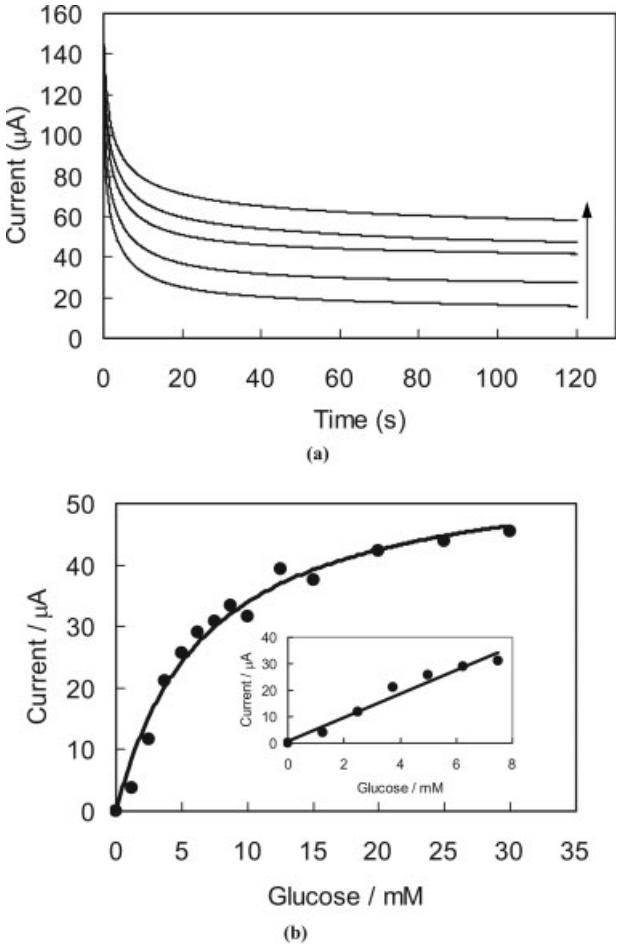

Figure 7. (a) Amperometric responses of the GOx-immobilized EFK16-II-modified HOPG electrode in 100 mM potassium phosphate buffer (pH 7.0) containing 0.2 mM FCA and various concentrations of glucose (from bottom to top, 2.5, 5, 10, 20 mM); (b) calibration curve for the GOx-immobilized EFK16-II-modified HOPG electrode. Inset shows the linear range of the calibration curve, $r^2 = 0.96$.

Stability

The storage stability of the ionic-complementary peptide-based GOx electrode was examined by measuring the currents for 20 mM glucose at 0.45 V during the cyclic voltammograms obtained on the first day and the 30th day following the initial preparation of the electrode. The electrode was kept at 4°C in 0.1 M phosphate buffer (pH 7.0) when not in use. The current obtained at 0.45 V decreases to about 87% of the original value after 1 month of storage. This loss in current is lower than that reported for GOx-modified dipeptide FF-modified gold electrodes, which were found to lose 40% of their activity within 2 weeks of storage.[15] This better long-term storage stability can be attributed to the good compatibility of the ionic-complementary peptide and GOx.

In addition, the ionic-complementary peptide-based GOx electrode shows good operational stability. This operational stability was indicated by negligible changes in peak currents after 50 repeated CV cycles between 0 and 0.5 V at 10 mV/s. This result also reflects the good adhesion of the peptide assemblies and GOx to the HOPG electrode.

In this work, HOPG was used as a model electrode to test the concept of using ionic-complementary peptide modified electrodes for (bio)molecular sensing. The presented results demonstrate promise for the use of ionic-complementary peptides to modify HOPG electrodes for biosensor applications. The presence of patterned peptide nanofibers can improve the wettability of the HOPG surface, but does not significantly increase the resistance to electron transfer. In addition, they provide functional groups, e.g., carboxylic and amine groups, for immobilizing enzymes and other sensing molecules such as antibodies or DNA. The good stability of the peptide nanofibers under various solution conditions and compatibility with the immobilized enzymes could make such peptides a promising new class of biomaterials for biomolecular sensing and for studying the electrochemistry of proteins. This work can also be easily extended to nanoelectrodes, such as carbon nanotube electrodes, which would be expected to show higher sensitivity and possible non-mediated amperometric responses. In addition, rational peptide sequence design, for example, through the introduction of aromatic residues, may further enhance interaction with the electrode and improve its electrochemical properties.

Conclusions

The ionic-complementary, self-assembling peptide EFK16-II was used to modify HOPG electrodes for enzyme-based biosensor applications. The peptide adsorbed and formed nanofibers, parallel or oriented 60° or 120° to each other, on the HOPG electrode surface. The presence of EFK16-II nanofiber assemblies decreased the water contact angle on the HOPG surface, indicating an enhanced wettability of the surface. The presence of the peptide nanofiber coating did not block electron transfer to the electrode, although some inhibition of the ferri-ferrocyanide reaction was observed at higher scan rates. GOx could be covalently immobilized onto the peptide nanofiber-modified HOPG electrode and then used as a glucose sensor. A linear amperometric response was observed up to 7.5 mM glucose. GOx immobilized on the self-assembled peptide nanofibers showed high affinity for glucose with an apparent Michaelis–Menten constant K_m of 6.8 ± 0.9 mM. The glucose biosensor also shows relatively good storage and operational stabilities. These results indicate that this ionic-complementary peptide as a surface modifier provides an interface for enzymes with relatively good biocompatibility. This study has demonstrated the promise for the use of ionic-complementary self-assembling peptides in modification of electrodes for (bio)molecular sensing and diagnostic applications.

Acknowledgments

Support for this research has been provided by the Natural Sciences and Engineering Research Council of Canada (NSERC), Canadian Foundation for Innovation (CFI), and the Canada Research Chairs (CRC) Program for one of the coauthors (PC). We also thank Tony Qian for his kind help on this project.

Literature Cited

1. Chaubey A, Malhotra BD. Mediated biosensor. *Biosens Bioelectron*. 2002;17:441–456.
2. Gorodetsky AA, Barton JK. DNA-mediated electrochemistry of disulfides on graphite. *J Am Chem Soc*. 2007;129:6074–6075.

3. Emregul E. Development of a new biosensor for superoxide radicals. *Anal Bioanal Chem*. 2005;383:947–954.
4. Basu M, Seggerson S, Henshaw J, Jiang J, Cordona RdA, Lefave C, Boyle PJ, Miller A, Pugia M, Basu S. Nano-biosensor development for bacterial detection during human kidney infection: use of glycoconjugate-specific antibody-bound gold nanowire arrays. *Glycoconjug J*. 2004;21:487–496.
5. Knichel M, Heiduschka P, Beck W, Jung G, Wolfgang G. Utilization of a self-assembled peptide monolayer for an impedimetric immunosensor. *Sens Actuators B*. 1995;28:85–94.
6. Terry LA, White SF, Tigwell LJ. The application of biosensors to fresh produce and the wider food industry. *J Agric Food Chem*. 2005;53:1309–1316.
7. Sungur S, Emregul E, Gunendi G, Numanoglu Y. New glucose biosensor based on glucose oxidase-immobilizaed gelatin film coated electrodes. *J Biomat Appl*. 2004;18:265–277.
8. Yemini M, Xu P, Kaplan DL, Rishpon J. Collagen-like peptide as a matrix for enzyme immobilization in electrochemical biosensors. *Electroanalysis*. 2006;18:2049–2054.
9. Delvaux M, Walcarius A, Demoustier-Champagne S. Bienzyme HRP-GOx-modified gold nanoelectrodes for the sensitive amperometric detection of glucose at low overpotentials. *Biosens Bioelectron*. 2005;20:1587–1594.
10. Zhang S, Wang N, Yu H, Niu Y, Sun C. Covalent attachment of glucose oxidase to an Au electrode modified with gold nanoparticles for use as glucose biosensor. *Bioelectrochemistry*. 2005;67:15–22.
11. Shervedani RK, Mehrjardi AH, Zamiri N. A novel method for glucose determination based on electrochemical impedance spectroscopy using glucose oxidase self-assembled biosensor. *Bioelectrochemistry*. 2006;69:201–208.
12. Gooding JJ, Erokhin P, Losic D, Yang W, Policarpio V, Liu J, Ho FM, Situmorang M, Hibbert DB, Shapter JG. Parameters important in fabricating enzyme electrodes using self-assembled monolayers of alkanethiols. *Anal Sci*. 2001;17:3–9.
13. Creager SE, Olsen KG. Self-assembled monolayers and enzyme elelctrodes: progress, problems and prospects. *Anal Chim Acta*. 1995;307:277–289.
14. Moore ANJ, Katz E, Willner I. Immobilization of pyrroloquinoline quinone on gold by carbodiimide coupling to adsorbed polyamines: stability comparision to attachment via a chemisorbed thiol monolayer. *Electroanalysis*. 1996;8:1092–1094.
15. Yemini M, Reches M, Gazit E, Rishpon J. Peptide nanotube-modified electrodes for enzyme-biosensor applications. *Anal Chem*. 2005;77:5155–5159.
16. Yemini M, Reches M, Rishpon J, Gazit E. Novel electrochemical biosensing platform using self-assembled peptide nanotubes. *Nano Lett*. 2005;5:183–186.
17. Zhang S, Holmes T, Lockshin C, Rich A. Spontaneous assembly of a self-complementary oligopeptide to form a stable macroscopic membrane. *Proc Natl Acad Sci USA*. 1993;90:3334–3338.
18. Zhang S, Lockshin C, Cook R, Rich A. Unusually stable β-sheet formation in an ionic self-complementary oligopeptide. *Biopolymers*. 1994;34:663–672.
19. Yang H, Fung SY, Pritzker M, Chen P. Surface-assisted assembly of an ionic complementary peptide: controllable growth of nanofibers. *J Am Chem Soc*. 2007;129:12200–12210.
20. Yang H, Fung SY, Pritzker M, Chen P. Modification of hydrophilic and hydrophobic surfaces using an ionic-complementary peptide. *PLoS One*. 2007;2:ei325–ei311.
21. Zhang S. Emerging biological materials through molecular self-assembly. *Biotechnol Adv*. 2002;20:321–339.
22. Fung SY, Yang H, Chen P. Formation of colloidal suspensions of hydrophobic compounds using an amphiphilic self-assembling peptide. *Colloids Surf B: Biointerf*. 2006;55:200–211.
23. Keyes-Baig C, Duhamel J, Fung SY, Bezaire J, Chen P. Self-assembling peptide as a potential carrier for hydrophobic compounds. *J Am Chem Soc*. 2004;126:7522–7532.
24. Davis ME, Michael Motion JP, Narmoneva DA, Takahashi T, Hakuno D, Kamm RD, Zhang S, Lee RT. Injectable self-assembling peptide nanofibers create intramyocardial microenvironments for endothelial cells. *Circulation*. 2005;111:442–450.
25. Kisiday J, Jin M, Kurz B, Hung H, Semino C, Zhang S, Grodzinsky AJ. Self-assembling peptide hydrogel fosters chondrocyte extracellular matrix production and cell division: implications for cartilage tissue repair. *Proc Natl Acad Sci USA*. 2002;99:9996–10001.
26. Semino CE, Merok JR, Crane GG, Panagiotakos G, Zhang S. Functional differentiation of hepatocyte-like spheroid structures from putative liver progenitor cells in three-dimensional peptide scaffolds. *Differentiation*. 2003;71:262–270.
27. Ellis-Behnke RG, Liang Y-X, You S-W, Tay DKC, Zhang S, So K-F, Schneider GE. Nano neuro knitting: peptide nanofiber scaffold for brain repair and axon regeneration with functional return of vision. *Proc Natl Acad Sci USA*. 2006;103:5054–5059.
28. Holmes TC, de Lacalle S, Su X, Liu G, Rich A, Zhang S. Extensive neurite outgrowth and active synapse formation on self-assembling peptide scaffolds. *Proc Natl Acad Sci USA*. 2000;97:6728–6733.
29. Long J, Chen P. Surface characterization of hydrosilylated polypropylene: contact angle measurement and atomic force microscopy. *Langmuir*. 2001;17:2965–2972.
30. Gooding JJ, Hibbert DB. Application of alkanethiol self-assembled monolayers to enzyme electrodes. *TrAC-Trends Anal Chem*. 1999;18:525–533.
31. Jun S, Hong Y, Immamura H, Ha B-Y, Bechhoefer J, Chen P. Self-assembly of the ionic peptide EAK16: the effect of charge distributions on self-assembly. *Biophys J*. 2004;87:1249–1259.
32. Casal HL, Kohler U, Mantsch HH. Structural and conformational changes of β-lactoglobulin B: an infrared spectroscopic study of the effect of pH and temperature. *Biochim Biophys Acta*. 1988;957:11–20.
33. Nakanishi T, Miyashita N, Michinobu T, Wakayama Y, Tsuruoka T, Ariga K, Kurth DG. Perfectly straight nanowires of fullerenes bearing long alkyl chains on graphite. *J Am Chem Soc*. 2006;128:6328–6329.
34. Klymchenko A, Furukawa S, Mullen K, Auweraer MVd, Feyter SD. Supramolecular hydrophobic–hydrophilic nanopatterns at electrified interfaces. *Nano Lett*. 2007;7:791–795.
35. Yang G, Woodhouse KA, Yip CM. Substrate-facilitated assembly of elastin-like peptides: studies by variable-temperature in situ atomic force microscopy. *J Am Chem Soc*. 2002;124:10648–10649.
36. Brown CL, Aksay IA, Saville DA, Hecht MH. Templated-directed assembly of a *de novo* designed protein. *J Am Chem Soc*. 2002;124:6846–6848.
37. Severin N, Okhapkin IM, Khokhlov AR, Rabe JP. Adsorption of polyelectrolyte molecules to a nanostructured monolayer of amphiphiles. *Nano Lett*. 2006;6:1018–1022.
38. Bard AJ, Faulkner LR. *Electrochemical Methods: Fundamentals and Applications*. New York: Wiley; 2001.
39. Heider GH, Sasso SV, Huang KM, Yacynych AM, Wieck HJ. Electrochemical platinization of reticulated vitreous carbon electrodes to increase biosensor response. *Anal Chem*. 1990;62:1106–1110.
40. Shan D, Zhu M, Xue H, Cosnier S. Development of amperometric biosensor for glucose based on a novel attractive enzyme immobilization matrix: calcium carbonate nanoparticles. *Biosens Bioelectron*. 2006;22:1612–1617.
41. Dong XD, Lu JT, Cha CS. Characteristics of the glucose oxidase at different surfaces. *Bioelectrochem Bioenerg*. 1997;42:63–69.
42. Delvaux M, Demoustier-Champagne S. Immobilisation of glucose oxidase within metallic nanotubes arrays for application to enzyme biosensors. *Biosens Bioelectron*. 2003;18:943–951.
43. Gooding JJ, Pugliano L, Hibbert DB, Erokhin P. Amperometric biosensor with enzyme amplification fabricated using self-assembled monolayers of alkanethiols: the influence of the spatial distribution of the enzymes. *Electrochem Commun*. 2000;2:217–222.

Manuscript received Sep. 28, 2007, and final revision Feb. 26, 2008.

BTPR070340P